^{19}F ligand hyperfine structure in the room-temperature electron-paramagnetic-resonance spectra of Mn^{2+} substituting for Zr^{4+} sites in $Cd_2ZrF_8 \cdot 6H_2O$ single crystals

Geetha Jayaram and V. G. Krishnan
Physics Department, Osmania University, Hyderabad 500007, India
(Received 12 July 1994; revised manuscript received 13 September 1994)

Electron-paramagnetic-resonance spectra of Mn^{2+} in single crystals of $Cd_2Zr\ F_8 \cdot 6H_2O$ have been recorded at room temperature. An abundance of ^{19}F ligand hyperfine structure has been observed for all the 30 Mn^{2+} hyperfine lines at all orientations of the crystals. From the angular-variation study of ^{19}F superhyperfine structure it has been concluded that the impurity ion shows a preferential occupation of ZrF_8^{4-} site over that of $[CdF_4(H_2O)_3]^{2-}$. This is due to the identical ionic radius of Zr^{4+} and Mn^{2+} (0.80 Å) while the Cd^{2+} ionic radius is much larger (0.99 Å). This is an instance where Mn^{2+} has replaced Zr^{4+} in a lattice where Cd^{2+} was available and an isostructural $Mn_2ZrF_8 \cdot 6H_2O$ was known to exist. A qualitative evaluation of the spin-Hamiltonian parameters has been carried out.

The interaction between a paramagnetic impurity and the magnetic moment of the ligand nuclei is observed in the EPR spectrum as an inhomogeneous broadening of the hyperfine lines due to the interaction of the unpaired electron with the nuclear spin of the ligand nuclei. However, in certain circumstances this interaction may be sufficiently large to cause structure on each of the hyperfine lines giving rise to superhyperfine structure (shfs). If the unpaired electron occupying a certain shell is shielded from the ligands by the outermost shells (as in rare-earth ions where the electrons in the $4f$ shell are shielded by the $5s$ and $5p$ shells), then the shfs is not resolved. Such difficulties are not encountered for the unpaired $3d$ electrons in the case of the iron group ions due to their occupation of the outermost shell which is fully exposed to the ligands.

Despite the observation of shfs in many cases, ^{19}F shfs in the EPR spectra of $(Mn)^{2+}$ was observed[1] only in 1971 in BaF_2, CaF_2, and SrF_2. Prior to this electron-nuclear double resonance was used[2] to investigate shfs below 77 K even when the interaction merely caused inhomogeneous broadening of the Mn^{2+} hyperfine (hf) lines. This was reported[3] for Mn^{2+}:CaF_2, where linewidths of ca. 30 G were attributed to the unresolved manganese-fluorine interaction as well as contributions from the loose coupling of Mn^{2+} (ionic radius $=0.80$ Å) and the larger Ca^{2+} (ionic radius $=0.99$ Å). The latter gives rise to large-amplitude local mode vibration, which can be reduced only by lowering the temperature.

Cd^{2+} and Ca^{2+} have the same ionic radius and hence the cadmium lattice serves as a good approximation for the calcium lattice. The main difference was in the low-symmetry pentagonal bipyramidal coordination of Cd^{2+} with four fluorines and three water oxygens in $Cd_2ZrF_8 \cdot 6H_2O$ as against the cubic symmetry with eight fluorines around the Ca^{2+} site in CaF_2. Here we report the well-resolved ^{19}F shfs at room temperature. $Cd_2ZrF_6 \cdot 6H_2O$ is extremely interesting as there are two possible substitutional sites for the Mn^{2+} ion (radius $=0.80$ Å), viz., Cd^{2+} ion (radius $=0.99$ Å) and Zr^{4+} ion (radius $=0.80$ Å) which is surrounded by eight fluorines in a distorted cubic arrangement (Fig. 1).

Crystals of $Cd_2ZrF_8 \cdot 6H_2O$ were grown by the action of freshly precipitated $CdCO_3$ on a solution of high-purity ZrO_2 in HF followed by slow evaporation at room temperature. It crystallizes[4] in the monoclinic crystal class with space group $B\ 2/b$ with $Z=4$ and cell dimensions $a=11.246$ Å, $b=12.594$ Å and $c=8.127$ Å, $\gamma=118.9°$. The structure is built up of layers of Cd and Zr polyhedra perpendicular to the b axis. The bond distances within the Cd and Zr polyhedra are given in Table I.

EPR spectra were recorded on a conventional X band (JEOL JES-RE3X) spectrometer with 100 kHz magnetic-field modulation. Spectra are recorded with the magnetic field rotating in (i) the ac plane and (ii) a plane perpendicular to the ac plane, viz., ab^* plane ($\mathbf{b}^* \perp \mathbf{a}$). In a general direction, the spectrum consisted of two sets of 30 lines ($Mn^{2+}, S=\frac{5}{2}, I=\frac{5}{2}$). Figure 2 (a) shows the spectrum with the magnetic field **H** along the principal axis of one of the sites. A striking feature was the clearly observed shfs on all the 30 hf lines. It was interesting to see that the shfs on each of the hf lines is the same for all the five fine-structure transitions indicating that the splitting was independent of the strength of the magnetic field.

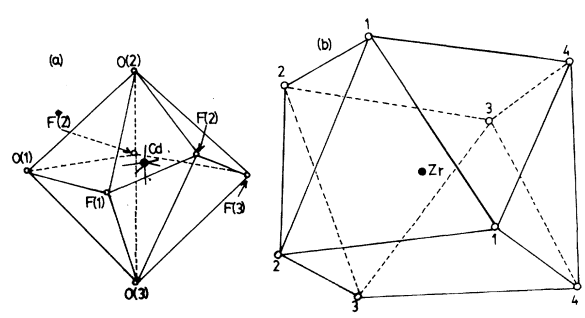

FIG. 1. Nearest-neighbor arrangement of atoms (a) around Cd^{2+} and (b) around Zr^{4+}.

TABLE I. The bond distances for Cd and Zr atoms.

Cd-F(1)	2.40 Å	Zr-F(1)	2.12 Å	(×2)
Cd-F(2)	2.44 Å	Zr-F(2)	2.13 Å	(×2)
Cd-F*(2)	2.68 Å	Zr-F(3)	2.12 Å	(×2)
Cd-F(3)	2.36 Å	Zr-F(4)	2.07 Å	(×2)
Cd-O(1)	2.44 Å			
Cd-O(2)	2.31 Å			
Cd-O(3)	2.36 Å			

This was in contrast to the observation in alkaline-earth fluorides with rare-earth impurities, where the resolution of shfs was found to depend not only upon the m_I-value within a fine-structure transition but the fine-structure transition itself.[2,5] In Mn^{2+}:Ba_2ZnF_6 the ^{19}F shfs was resolved for four out of the six hf lines within the central $-\frac{1}{2}\leftrightarrow+\frac{1}{2}$ fine-structure transition.[6]

We summarize our results by describing the basic features of the spectra by the spin Hamiltonian

$$\mathcal{H}=g\beta HS+SDS+AIS+\sum_i ST_iI_i^F$$

where the first term is the electronic Zeeman term, the second term represents the crystal field, the third corresponds to the hyperfine interaction of the ^{55}Mn nucleus. The last term under the summation describes shf interaction with eight nearest-neighbor ^{19}F nuclear spins ($I=\frac{1}{2}$). The strength of the shf interaction is characterized by the tensor T, whose form is determined by the symmetry of the nuclear spin involved. In $Cd_2ZrF_8\cdot 6H_2O$, Cd^{2+} has four fluorines as nearest neighbors and Zr^{4+} has eight. Because of the extreme complexity of the EPR spectra due to the shf interaction, it is not possible in general to make a straightforward analysis. We assume that the ^{19}F sites have axial symmetry thereby restricting T to two components, $T_\parallel$ and $T_\perp$. The parallel axis of the tensor lies along the Mn-F direction. The quadrupole interac-

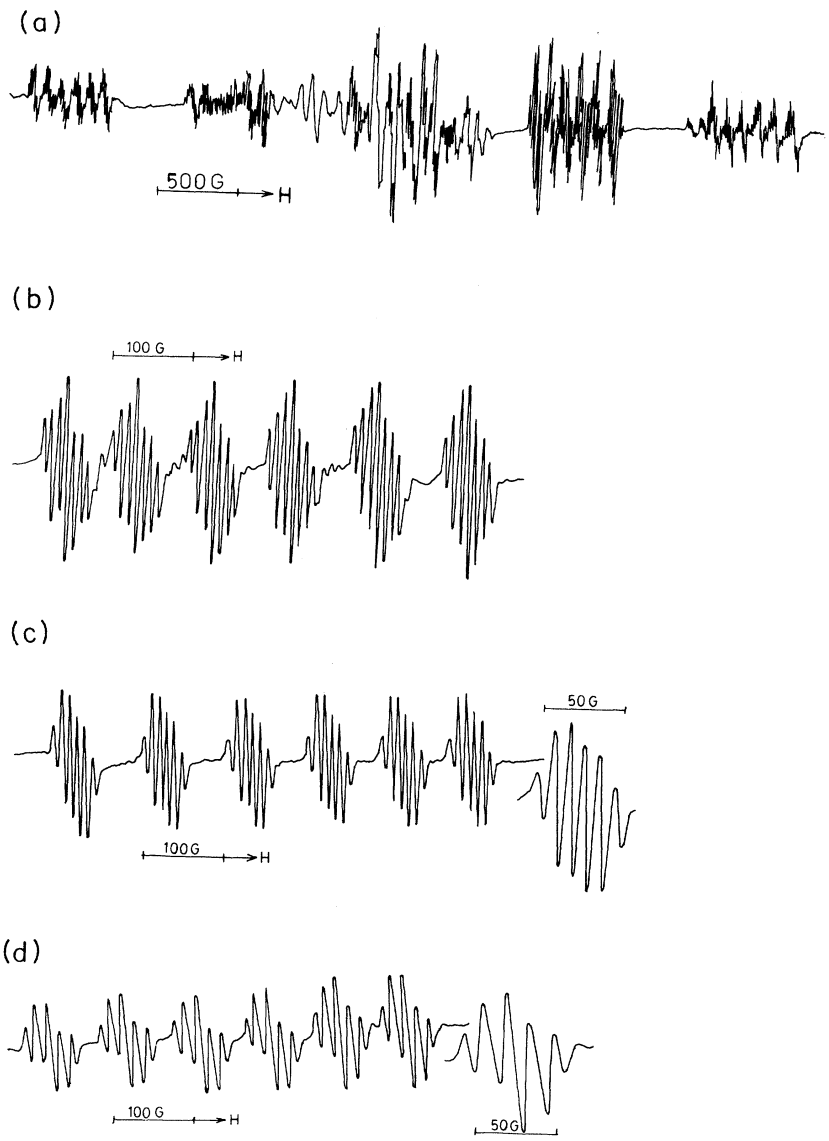

FIG. 2. EPR spectra for Mn^{2+}: $Cd_2ZrF_8\cdot 6H_2O$ with (a) **H** along the principal axis of one of the sites, (b) shfs on the hyperfine lines for $-\frac{5}{2}\leftrightarrow-\frac{3}{2}$ fine-structure transition along the principal axis, (c) shfs at ca. 20° away from the principal axis, and (d) shfs at ca. 30° away from the principal axis.

tion has not been included due to the above-mentioned complexity. However, if a Q-band study is carried out it would be possible to incorporate and analyze the quadrupole interaction.

We now visualize the spectra that would be observed if Mn^{2+} were to replace the (i) Cd^{2+} or (ii) Zr^{4+} site.

(i) In the CdF_4O_3 polyhedron, the CdF_4O plane is almost perpendicular to the ac plane. The line joining Cd to the two apical oxygens is perpendicular to the CdF_4O plane and hence lies in the ac plane. These are the shortest among all the seven Cd-F and Cd-O distances. If **H** is oriented along the shortest Cd-O distances, the three fluorines would have to be considered inequivalent. This is because of the deviation from orthogonality of the F-Cd-F and F-Cd-O bond angles. In addition the shfs would be small due to the large Cd-F bond distances (Table I). Therefore a maximum of only four shf lines should be observed. The observed spectra [Figs. 2(a)–2(d)] clearly eliminated Cd^{2+} as an occupation site for the Mn^{2+} ion. This was surprising in view of the existence of an isostructural $Mn_2ZrF_8 \cdot 6H_2O$.[7]

(ii) The ZrF_8 polydedron is oriented so that the c axis trisects the plane formed by the three fluorines, viz., F(1)F(4)F(4) and could therefore be considered the principal axis of the distorted cube. The maximum of the zero-field splitting occurs very close to this direction [Fig. 2(a)]. Each of the ^{55}Mn hf lines is then split into nine components due to the interaction with the eight fluorines (intensity ratio being 1:8:28:56:70:56:28:8:1) [Fig. 2(b)]. When the magnetic field is rotated ca. 20° away from the principal axis, the projection on the ac plane shows only five equivalent fluorines. This would require a six-line fluorine shfs and a further splitting into three components due to two inequivalent fluorines, whose projection on the ac plane does not coincide. But the large linewidth of ca. 4.5 G, did not permit this resolution [Fig. 2(c)]. Further rotation of 10° showed four equivalent fluorines which would give rise to a five-line shfs and three inequivalent fluorines which would further split the above lines into four components [Fig. 2(d)].

The spectra shown in Figs. 2(a)–2(d) clearly indicate that the paramagnetic impurity preferred to replace the Zr^{4+} site. This replacement required charge compensation which could either raise or lower the site symmetry. As the polyhedron is already highly distorted it was difficult to estimate the effect of the charge compensation except noting that $|E/D| > 0.5$. The arrangement of eight fluorines around Zr^{4+} also suggested the possibility of two ZrF_4 tetrahedra. The hyperfine splitting of 101 G immediately ruled out this possibility.

Identical splittings were recorded for the $\pm\frac{5}{2} \leftrightarrow \frac{3}{2}$ and $\pm\frac{3}{2} \leftrightarrow \pm\frac{1}{2}$ fine-structure transitions in the angular variation study. The $+\frac{1}{2} \leftrightarrow -\frac{1}{2}$ region was, however, overcrowded with lines due to the second site, forbidden lines due to the large rhombic component of the zero-field splitting tensor. The $T_{\parallel}$ values were evaluated using the spectra shown in Figs. 2(b)–2(d). The $T_{\perp}$ splittings were then measured by rotating the magnetic field by 90° from each of the above directions in the ac and ab^* planes. Along with the spectra observed in the ab^* plane the spin-Hamiltonian parameters were evaluated and are given below:

$$g = 2.0005 + 0.005, \quad F(4)\ T_{\parallel} = 13.6\ G, \quad F(4)\ T_{\perp} = 3\ G\ ,$$

$$A = -101 + 2.0\ G, \quad F(3)\ T_{\parallel} = 9.5\ G, \quad F(3)\ T_{\perp} = 3\ G\ ,$$

$$D = -330.6\ G, \quad F(2)\ T_{\parallel} = 9.5\ G, \quad F(2)\ T_{\perp} = 3\ G\ ,$$

$$E = 180.5\ G, \quad F(1)\ T_{\parallel} = 9.0\ G, \quad F(1)\ T_{\perp} = 3\ G\ .$$

Unfortunately, the complexity of the spectra in all directions prevented any possibility of seeking a theoretical fit to the experimental observations. A Q-band study would be able to provide the precise orientations of the various superhyperfine tensors.

We thank Professor K. Rama Reddy for encouragement. We also thank K. Balarama Murty and N. Saratchandran (Nuclear Fuel Complex) for providing us with high-purity ZrO_2. Thanks are also due to C.I.L., University of Hyderabad for allowing the use of their EPR spectrometer facility.

[1]R. J. Richardson, S. Lee, and T. J. Menne, Phys. Rev. B **4**, 3837 (1971); T. J. Menne, S. Lee, and R. J. Richardson, *ibid.* **6**, 1065 (1972).

[2]H. Bill, Phys. Lett. A **29**, 593 (1969), and references therein.

[3]R. A. Serway, Phys. Lett. A **26**, 642 (1968); R. Calvo and R. Orbach, Phys. Rev. **164**, 284 (1967).

[4]M. F. Eibermann, T. A. Nadalova, R. L. Davidovich, G. F. Levichishina, and B. V. Bukvetskii, Koord. Khim. **6**, 1885 (1980).

[5]S. Lee, A. J. Bevolo, and Chi-Shung Yang, J. Chem. Phys. **60**, 1628 (1974).

[6]A. B. Vassilikou, H. Matthies, K. Recker, F. Wallrafen, and G. Lehmann, Phys. Status Solidi B **155**, K59 (1989).

[7]L. P. Otroschenko, R. L. Davidovich, V. I. Simonov, and N. V. Belov, Sov. Phys. Crystallogr. **26**, 675 (1981).